Erbium:YAG Laser Ablation of Retinal Tissue under Perfluorodecaline: Determination of Laser–Tissue Interaction in Pig Eyes

Thomas Wesendahl,[1] *Peter Janknecht,*[1] *Bea Ott,*[2] *and Martin Frenz*[2]

Purpose. To evaluate the effect of Er:YAG laser on pig retina using a perfluorodecaline/retina interphase with the goal of precisely determining the extent of retinal tissue ablation.

Methods. Free running (τ = 250 μsec) Er:YAG laser pulses were transmitted through a zirconium fluoride (ZrF_4) fiber guarded by quartz rod (d = 1000 μm). Laser pulses were applied to the retinal surface of enucleated pig eyes. Eyes were mounted in a specially designed rotating sample holder. The fiber probe was elevated 1.0 ± 0.3 mm above the retinal surface with perfluorodecaline serving as transmitting medium. The laser energy was applied in a circular pattern with a radius of 3.0 mm. Radiant exposures were set to 1, 3, 5, and 10 J/cm^2.

Results. Tissue ablation linearly increased with radiant exposure from 3.2 ± 3.7 μm at 1 J/cm^2 up to 40.9 ± 12.9 μm at 10 J/cm^2. Thermal tissue changes extended 70 ± 10 μm vertically into the retina and 25 ± 5 μm horizontally. Distortion of outer photoreceptor segments was noticed when the retina was exposed to radiant exposures of 3 J/cm^2 or higher.

Conclusions. The Er:YAG laser in combination with perfluorodecaline produced precise ablation of the pig retina, which suggests the feasibility of this technique for safe ablation of epiretinal membranes. (*Invest Ophthalmol Vis Sci.* 2000;41:505–512)

Membranes that develop on the inner surface of the retina (epiretinal membranes) occur under a number of circumstances, including proliferative retinopathy, ocular inflammation, nonproliferative vascular disorders, after penetrating injury, associated with rhegmatogenous retinal detachment, after successful retinal reattachment, retinal photocoagulation, cryotherapy, and as an idiopathic condition in otherwise healthy eyes.[1–3] These membranes often exert traction on the underlying retina, causing visual impairment or tractional detachment of the macula.[4]

Currently, the common method of treatment is an attempt to remove these membranes from the retinal surface by engaging the edge and peeling it off with a microforceps.[5–8] However, this technique frequently does not result in complete removal because the membrane strongly adheres to the retina. A retinectomy of the area surrounding the membrane is performed to release the tractional forces on the retina. When a retinectomy is done, a retinal opening is produced that exposes the vitreous cavity to pigment epithelial cells, which are a major cause of proliferative retinopathy.[3,4,6,9] It would be desirable to be able to ablate membranes without exerting traction on the retina.

From 1994 to 1996, Brazitikos, D'Amico, and associates performed extensive research on the application of the Er:YAG laser in retinal and vitreous surgery. In 1995, Brazitikos et al. published an outstanding paper on Er:YAG laser surgery of the vitreous and the retina and reported on the possible use of perfluorochemicals with the Er:YAG laser. They concluded that the Er:YAG laser is an effective tool for the complete transection of vitreous membranes as well as the creation of retinectomies in detached retina. In epiretinal membrane surgery some problems have been reported.[10–13]

However, the Er:YAG laser has been shown to produce precise tissue transection and ablation.[14–19] The main problem in using infrared-laser (IR-laser) radiation in an aqueous environment such as the vitreous is the formation of fast expanding and subsequent collapsing water vapor bubbles at a submerged fiber tip and thereby the generation of strong pressure transients.[20–22]

The intention of the present study therefore was to systematically evaluate the effects of Er:YAG laser radiation on the pig retina using a perfluorodecaline/retina interphase.

Materials and Methods

Laser

A flashlamp-pumped Er:YAG laser emitting light at a wavelength of 2.94 μm was used in free running mode. The laser emitted bursts of spikes at a repetition rate of 1.7 Hz with a pulse length of 250 μsec. A single spike duration lasted approximately 0.5 to 1 μsec and was separated from the following spike by 2 to 5 μsec. The laser energy was delivered onto

From the [1]Department of Ophthalmology, University of Freiburg, Germany; and [2]the Institute of Applied Physics, University of Berne, Switzerland.

Supported in part by the Forschungskommission der Albert-Ludwig Universtität Freiburg and by the Swiss Commission of the Encouragement of Scientific Research.

Submitted for publication April 26, 1999; revised September 15, 1999; accepted September 23, 1999.

Commercial relationships policy: Cc5.

Corresponding author: Peter Janknecht, Department of Ophthalmology, University of Freiburg, Kilianstrasse 5, D-79106 Freiburg, Germany. janknecht@aug.ukl.uni-freiburg.de

Copyright © Association for Research in Vision and Ophthalmology

Downloaded from tvst.arvojournals.org on 08/11/2022

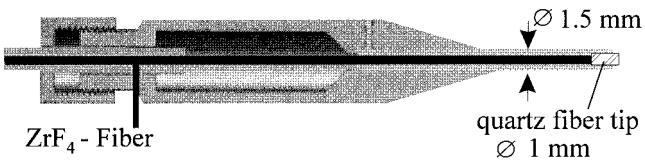

FIGURE 1. Schematic picture of the laser radiation delivery handpiece.

the retinal surface via a flexible zirconium fluoride (ZrF_4) fiber with a core diameter of 350 μm. A low-OH quartz fiber rod with a tip diameter of 1000 μm was coaxially mounted at the distal fiber end to protect the brittle and hygroscopic ZrF_4 fiber from damage.[23] Output energy of the individual laser bursts was adjusted from 7.85 to 78.5 mJ, resulting in a radiant exposure on the retinal surface of 1 to 10 J/cm^2. The fiber delivery system was incorporated into a sterilizable handpiece (Fig. 1). Laser radiation was unfocused and emitted from the fiber tip diverging at an angle of 12°.

Target Tissue

Twelve freshly enucleated pig eyes available from the local abattoir were used in this study. The eyes were randomly assigned to four treatment groups. Each group consisted of three eyes that were treated with a radiant exposure of either 1, 3, 5, or 10 J/cm^2. Within 4 hours after enucleation, the eyes were sectioned at the equator. The posterior segment containing the retina and the vitreous body was used for the laser experiment. Before removing the vitreous with a cotton swab, air was injected into the vitreous with a miniature cannula to produce a posterior vitreous detachment, which greatly facilitated the removal of the vitreous body. The posterior cup was then centered in a specially designed eye holder. A vacuum was applied to secure the posterior cup in place and to create a smooth bowl-shaped retinal surface.

All experiments were performed with a fluid/retina interphase. The eye cavity was filled with perfluorodecaline (DK-Line, Opsia Laboratoires) fluid, routinely used as an intraoperative nonpermanent vitreous substitute. It also has a low absorption coefficient at 2.94 μm (μ_a = 0.5 cm^{-1}) allowing the transmission of Er:YAG laser radiation.

Laser Experiments

The eye holder, with the eye cup, was centered on a rotating aluminum plate that was attached to the axle of an electric motor rotating at a speed of 1.88 rpm (Fig. 2). The laser delivery system was securely fastened to a metal arm above the eye, while the tip of the probe was immersed in perfluorodecaline.

To create a continuous circle of laser ablations, the fiber tip was first aligned with the center of the posterior segment followed by a decentration of 3 mm away from the center of the axle of the eye holder. By revolving the retinal cup underneath the fiber tip, a circle with a radius of 3 mm was created. The retina was exposed to single laser bursts emitted at a repetition rate of 1.7 Hz such that a 50% overlap of two consecutive laser spots was achieved (see Fig. 2). Radiant exposure was adjusted according to the different treatment groups (i.e., either 1, 3, 5, or 10 J/cm^2).

The macroscopic visible changes on the retina were recorded on videotape. In addition, fast flash video-shadow photography (illumination time t = 20 nsec) was used in a separate experiment (Fig. 3) to document the laser tissue interaction at the time of the laser impact on the retina. For that reason, the retina was cut into small flat pieces, necessary for taking images at the perfluorodecaline-retina interface.

The laser-induced pressure transients were simultaneously recorded using a piezoelectric polyvinylidene fluoride needle hydrophone. The hydrophone permitted measurements of pressure amplitudes in the range between 100 mbar and several kilobars.

Measurements of Distance between Fiber Tip and Retina

An identical setup environment was used in five different pig eyes to determine variations in distance from the tip of the laser fiber to the surface of the retina along the predetermined path of laser spots. For these measurements the laser handpiece was replaced by a standard ophthalmic A-scan biometry probe connected to a Technomed digital A-scan A5500 ultrasound unit. The ultrasound probe was immersed into the perfluorodecaline at a distance of 3 mm from the revolving axis of the eye holder and approximately 1 mm above the retinal surface. A total of 16 measurements were taken along the circular path per eye.

Sample Preparation

After laser irradiation, perfluorodecaline was removed and the posterior eye segment submerged in a combination of 4% buffered formaldehyde and 4% buffered glutaraldehyde (Kar-

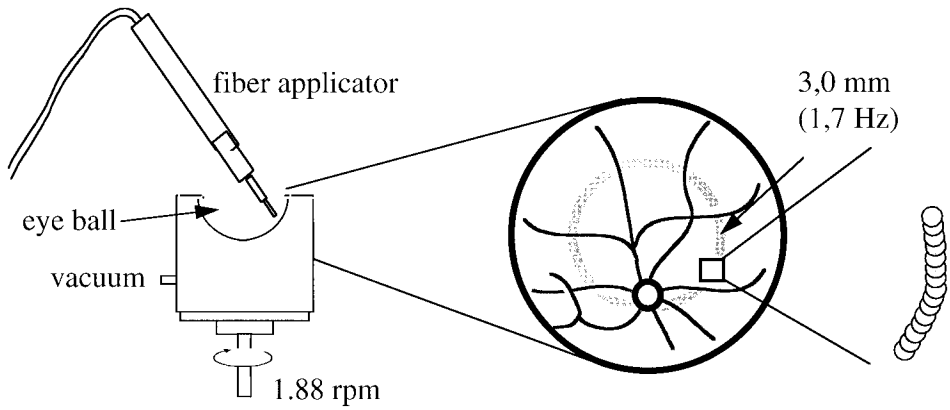

FIGURE 2. Laser experiments: Schematic drawing showing the experimental setup and the pattern of laser application. The laser energy was delivered on a circular path with a 3-mm radius. The individual laser spots were applied in such a way that a 50% overlap of the individual spots was achieved.

Downloaded from tvst.arvojournals.org on 08/11/2022

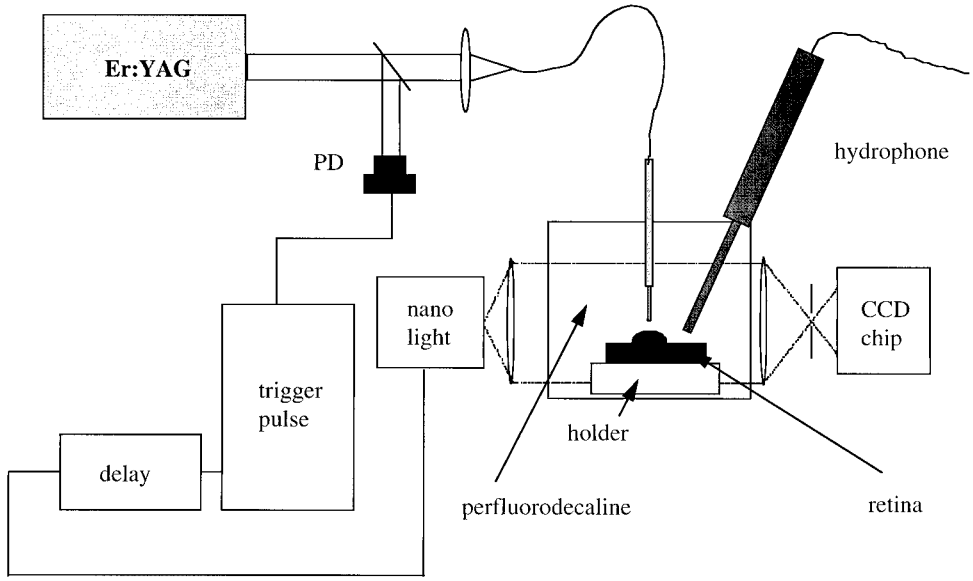

FIGURE 3. Schematic drawing of the fast flash shadow imaging. The flash light is controlled by the Er:YAG laser via a trigger/delay unit. A CCD chip records the shadow image. A needle hydrophone was used to measure laser-induced pressure transients at a distance of 2 mm to the fiber tip.

nowskys fixative) for 15 to 20 minutes to achieve rapid and proper fixation of the retina followed by storage in 4% buffered formaldehyde for a minimum of 48 hours.

If artificial retinal detachment occurred, the specimen was embedded after prefixation in an agar gel using a 2.5% agar solution. To cover the eye on all sides, the segment was placed in a small metal container, and liquid agar was poured into the eye until the entire container was filled. After cooling, the agar hardened to a mechanically solid gel, and the specimen was placed in 5% buffered formaldehyde for a minimum of 48 hours.

For microscopic examination, a disc containing the optic nerve head, the posterior pole, and the circular path of laser applications was cut from the eye cup using a 13-mm trephine. The disc was then sectioned along the vertical diameter and stained with Masson trichrome.

Measurement of Ablation Depth

Ten to 12 light microscopic sections were made from each tissue sample and examined under a routine light microscope (Olympus BH2). Laser-induced changes were identified using low-power fields (×4–×10). Measurements of the horizontal extension of the tissue ablation were performed with a measuring ocular (Olympus Θ WHK ×10/20 L) using a low-power field (×10). Measurement of the vertical ablation depth was carried out using a drawing attachment (Olympus BH2-DA). This allowed for the simultaneous observation of the histologic section and a drawing tablet located next to the microscope. An outline of characteristic retinal layers (internal limiting membrane, ILM; outer nuclear layer, ONL) could be sketched on paper (Fig. 4). After calibration, the distance between the ILM and the ONL was determined using a millimeter scale. For each slide, sketches of normal retina and ablated retina were drawn, and 17 measurements 1-cm apart were taken for normal and ablated retinas. The mean distances and the difference in the measurements between normal and treated retina were calculated and mathematically transformed into the retinal ablation depth. For each treatment group a total of 33 laser spots and corresponding normal retinal areas were measured and compared.

To determine the accuracy of the measurements, five sketches were drawn from an identical area of the retina. Measurements were taken according to the description above. The mean distance between the ILM and the ONL, the SD, and the SEM were calculated.

RESULTS

Measurements of Distance Variation

The measurements obtained with the ultrasound probe were used to estimate the variation in distance from the fiber to the retina. The distance was measured at 16 different locations indicated in Figure 5. These measurements showed the distance to be between 0.84 and 1.11 mm (mean, 1.02 ± 0.22 mm). Over the optic nerve head the distance was reduced to an average of 0.45 mm (Fig. 5).

Based on these ultrasound measurements, the distance between the fiber tip and the retina was assumed to be 1.0 ± 0.3 mm.

Accuracy of Light Microscopic Measurements

The mean distance between the ILM and the ONL was calculated to be 4.1829 ± 0.0192 mm, corresponding to a retinal distance of 103.2 ± 0.47 μm. The SEM was determined to be 0.212 μm.

Laser Experiments

The surface of the retina that underwent laser exposure changed transparency to a whitish-gray discoloration. This effect became more visible with higher energies. Using a high magnification (×6–×7), it was noticed that the surface of whitened areas appeared rough and irregular. Small membranous flakes protruded from the surface of the retina, whereas some areas exhibited a relatively smooth whitish surface. Almost simultaneously with the laser pulse, small bubbles visible to the naked eye emerged from the retina, ascending to the surface of perfluorodecaline. Adhesion of such bubbles to the tip of the fiber was sometimes followed by a more intense laser burst. During our experiments the perfluorodecaline did not

Downloaded from tvst.arvojournals.org on 08/11/2022

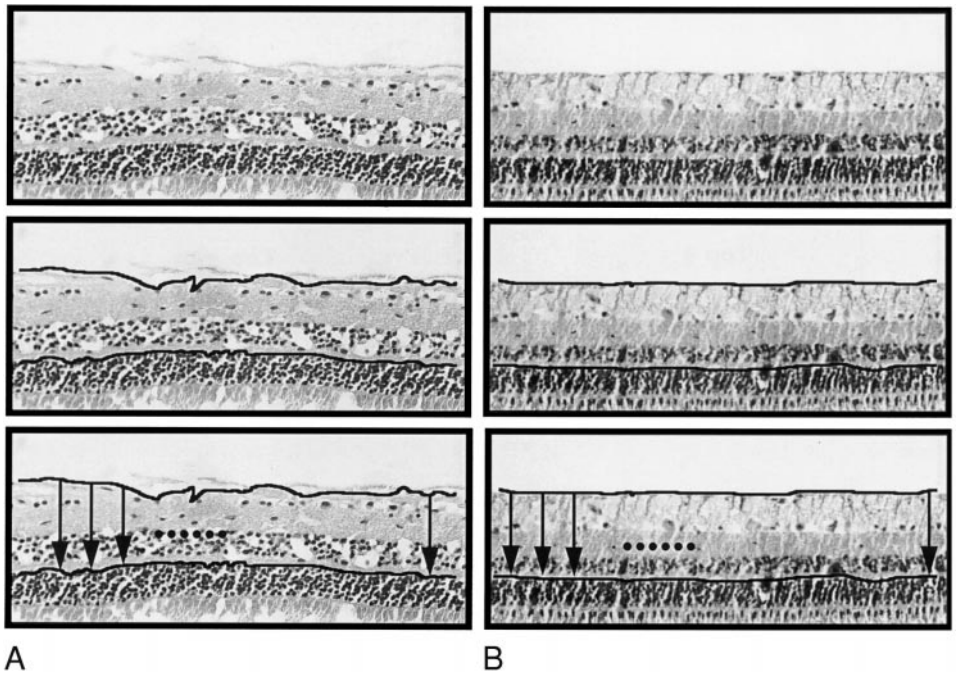

FIGURE 4. Illustration of the measuring procedure. The retinal surface and the internal border of the outer nuclear layer are outlined. The distance between those two lines is measured and recorded in a spread sheet. The difference between measurements from "normal" (**B**) and laser-irradiated retina (**A**) and the mean difference is calculated.

exhibit noticeable clouding or an accumulation of bubbles at the air–perfluorodecaline interphase. Visibility of the retinal surface was unimpaired at all times.

The fast flash photography revealed the creation of a vapor bubble at the surface of the retina (Fig. 6). Occasionally, a vapor bubble was noticed within the perfluorodecaline liquid projecting from the tip of the fiber toward the retinal surface. The bubbles were relatively small and their expansion and collapse slow. No pressure transients were measurable even at radiant exposures of 10 J/cm^2. In case perfluorodecaline was replaced by water, pressure transients between 45 ± 5 bars (1 J/cm^2) and 132 ± 20 bars (10 J/cm^2) visualizing the collapse of the water vapor channel were recorded (Fig. 7).

Light Microscopy

Qualitative Aspects. Tissue damage and ablation showed certain patterns characteristic of the corresponding energy levels. One J/cm^2 caused the ILM and the adjacent foot plates of the Mueller cells to be either missing, ruptured, or thermally damaged (Fig. 8A). The integrity of the retina, peripheral to the laser damage, was undisturbed. Radiant exposures of 3 and 5 J/cm^2 displayed similar conditions. The ILM and the foot plates of the Mueller cells were completely missing (Figs. 8B, 8C). The nerve fiber layer showed some loss of thickness, and the ganglion cell layer was vacuolated. In addition, the photoreceptor outer segments seemed to be displaced away from the center of the laser spot and often appeared disorganized. This phenomenon was more distinct with higher radiant exposures. At 10 J/cm^2 the retinal changes were much more prominent. Besides the ILM and the Mueller cell processes, the nerve fiber layer, and in most cases the ganglion cell layer, too, were missing. In addition, the retina was often detached from the pigment epithelium, resulting in retinal folds (Fig. 8D). There were also areas that exhibited an even deeper ablation of retinal tissue down to the photoreceptor region.

Quantitative Aspects. The horizontal extension of the areas of laser ablation measured 800 to 850 μm in length. Depth measurements taken at various locations showed that tissue ablation increased proportionally with the radiant exposure (Fig. 9). A tissue ablation depth of 3.2 ± 3.7 μm was

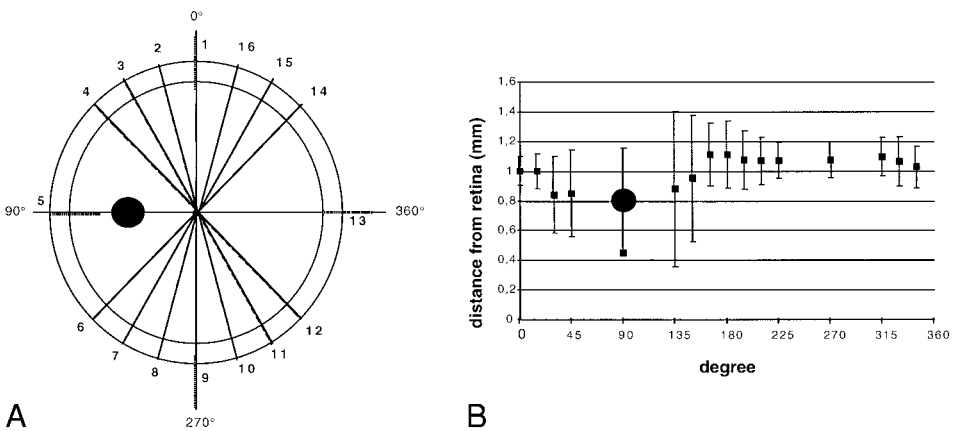

FIGURE 5. (**A**) Schematic drawing illustrating the measurement of the fiber–retina distance. Measurements were taken at 16 different locations indicated by the numbers 1 to 16. (**B**) Graphical illustration of the results of the distance measurement. Error bars represent SD. *Large black dot* represents the optic disc.

Downloaded from tvst.arvojournals.org on 08/11/2022

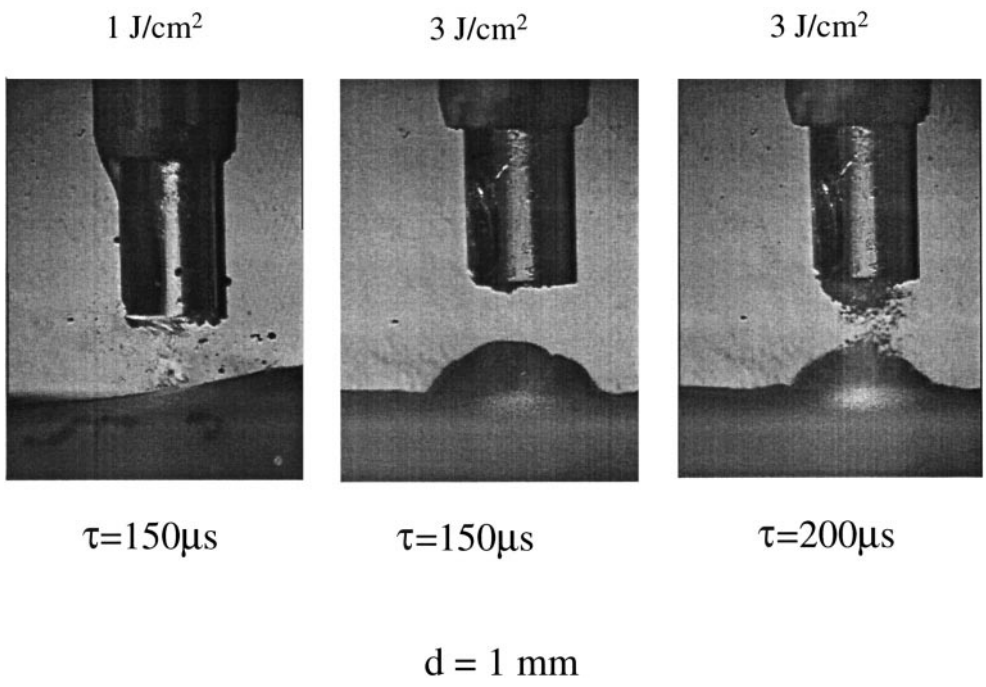

FIGURE 6. Shadow images of laser impact on retina under perfluorodecaline. The distance between the fiber and the tissue surface was 1 mm. Fiber diameter = 1 mm. At a radiant exposure of 1 J/cm^2 the ablation products are clearly visible. At 3 J/cm^2 a vapor bubble formed on the tissue surface. If ejected, tissue material adhered to the distal fiber tip, an additional small water vapor bubble formed at the fiber tip (τ = 200 μsec).

produced with 1 J/cm^2. At 3 J/cm^2, tissue ablation extended 9.9 ± 7.0 μm into the retina. At 5 J/cm^2 the resulting ablation depth measured 19.2 ± 6.4 μm, and at 10 J/cm^2 tissue ablation reached 40.9 ± 12.9 μm. Thermal damage judged by changes in tissue coloration extended 70 ± 10 μm into the retina and 25 ± 5 μm sideways. However, thermal tissue changes were difficult to determine and could not be quantified in all samples and sections examined.

DISCUSSION

Retinal microsurgery has become a widely used procedure in ophthalmic surgery. Today mechanical instruments such as scissors, forceps, hooks or subretinal injection of viscoelastic materials are the backbone of vitreoretinal surgery. However, submicroscopic dimensions of vitreous and retinal structures limit their field of application. Additionally tissue engagement by these mechanical techniques may produce retinal damage.[8]

The introduction of new laser instruments seems to be an appealing approach to improve vitreoretinal surgery and promises to overcome several problems that are related to conventional instruments. Lasers operating in the infrared part of the spectrum have several advantages over ultraviolet lasers used for retinal ablation in the past.[24,25] IR-lasers are solid state, rendering them more compact and less costly to operate than excimer lasers.[26] In addition, they do not inherit the potential risk of mutagenic effects compared with ultraviolet wavelengths.

The wavelength of an Er:YAG laser emitting at 2.94 μm corresponds to a maximum absorption peak of water that was shown to be around 10,000 cm^{-1}. Such high absorption translates into an optical penetration depth in water of 1 μm, making it impossible to transmit Er:YAG radiation through the cornea and the vitreous. Because of the high absorption in water, a fiber delivery system is mandatory to irradiate retinal tissue. Fiber delivery systems suitable for infrared radiation are sapphire and zirconium fluoride. Both materials can be built into a flexible fiber. A fiber delivery system using a flexible zirconium fluoride fiber guarded by a low OH quartz at the distal tip combines an acceptable rate of transmission (≈70% through a fiber 2 m in length).

Laser Experiments

We performed Er:YAG laser experiments on pig retinas to examine the efficacy and accuracy of partial retinal surface ablation using a flexible ZrF_4 fiber, and perfluorodecaline as transmitting medium. The retina was selected as a model tissue to examine potential applications of the Er:YAG laser for vitreoretinal surgery. Ablation of the inner layer of the retina provided a useful model for the ablation of thin epiretinal membranes.

Perfluorodecaline was selected as a transmitting fluid for two major reasons. First, many cases of vitreoretinal surgery, in particular complicated cases, are performed using perfluorodecaline as a temporary vitreous substitute. In these cases perfluorodecaline is used to facilitate surgical maneuvers on a mobile detached retina. Second, perfluorocarbon compounds such as perfluorodecaline exhibit an acceptable transmission rate for infrared radiation (absorption coefficient μ_a [2,94 μm] = 0.5 cm^{-1}) and can therefore be used as a transmitting medium for Er:YAG radiation.[27] This is especially important because the Er:YAG laser radiation causes a violently expanding and subsequently collapsing water vapor bubble at the distal fiber tip in an aqueous environment.[20] The formation and the collapse of the vapor bubble have been shown to be associated with the emission of strong pressure transients (Fig. 7). However, in water this vapor bubble is essential for a successful ablation of tissue because it establishes a delivery path for the highly absorbed infrared radiation through the water.[28]

To avoid any vapor bubble–induced damage to the retina, the aqueous environment was replaced by perfluorodecaline.

Downloaded from tvst.arvojournals.org on 08/11/2022

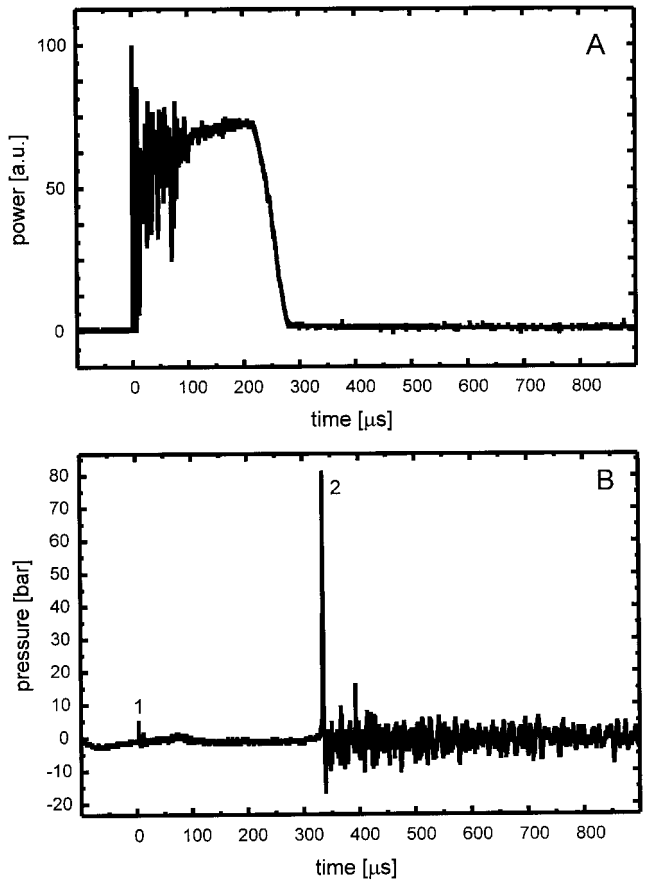

FIGURE 7. (**A**) Temporal power profile of the Er:YAG laser pulse. (**B**) Corresponding pressure signal measured in water. *1* indicates pressure transient caused by the explosive formation of the vapor bubble, *2* indicates pressure transient generated by the collapse of the vapor bubble. The pressure amplitudes were extrapolated up to the collapse center assuming that the amplitude of a spherical acoustic wave is inversely proportional to the distance (r) from the center. (radiant exposure H = 5 J/cm^2, fiber diameter = 1 mm.)

In fact, the flash photography revealed only a small vapor bubble on the surface of the retina, and pressure recordings within perfluorodecaline showed amplitudes of less than 100 mbar at a distance of 2 mm away from the fiber tip. The creation and the collapse of these small bubbles do not correspond to the bubbles created in water.[27] Instead, they are characterized by the disruption and vaporization of tissue and expulsion from the surface of the retina. The creation and collapse of these bubbles is much slower than those seen in an aqueous environment, supporting the fact that no pressure transients were measurable.

Despite these advantages, several disadvantages of perfluorodecaline have been reported in the literature,[13] including damage to the underlying retina in an attempt to dissect epiretinal membranes and rapid opacification of the perfluorodecaline liquid due to circulating ablation debris and accumulation of bubbles. Our experiments did not exhibit any noticeable clouding of perfluorodecaline. To the contrary, visibility of the retina was unimpaired at all times, and the transmission of perfluorodecaline used even after multiple extensive ablations decreased only to a small extent. Although bubble formation was noted with laser bursts at the surface of the retina, accumulation did not occur in our experiments.

Sample Preparation

Fixation of laser-exposed posterior pig eye segments in Karnowsky's fixative proved to have several advantages over the routinely used formaldehyde fixative. Benefits were a faster fixation of the retina and favorable staining characteristics when used in combination with Masson trichrome stain. The rapid fixation of the retinal tissue was able to reduce artificial retinal detachment. In addition, the internal vitreoretinal border region with the ILM and the radial fibers of the Mueller cells were much more clearly visible with the Masson trichrome stain after fixation in Karnowsky's fixative compared with formaldehyde fixation.

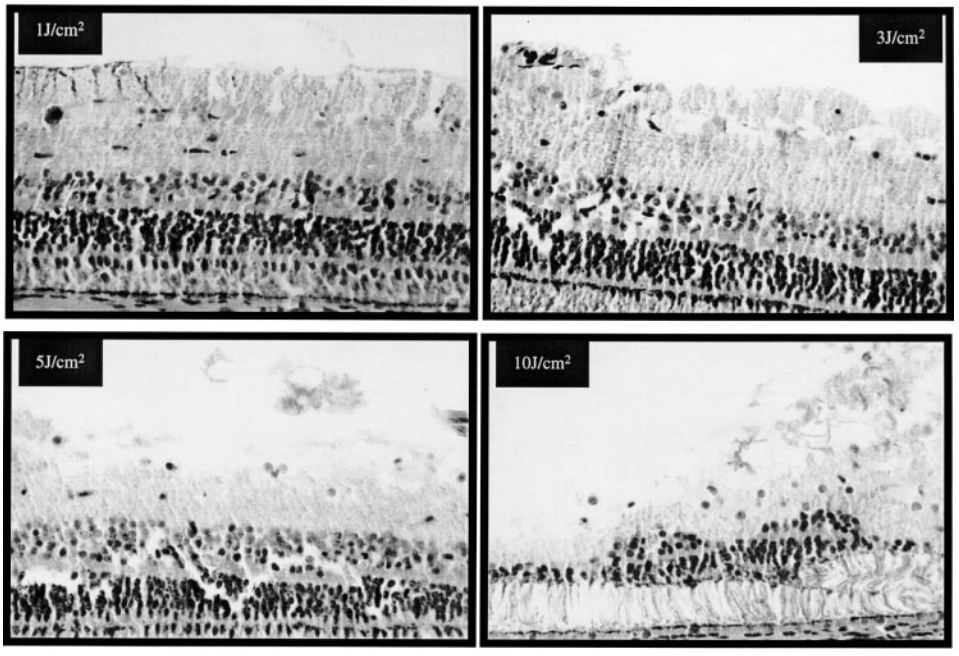

FIGURE 8. Microscopic photographs from laser-exposed retina with representative lesions induced by the Er:YAG laser. Note the differences in ablation depth produced by the different energies applied to the retina.

Downloaded from tvst.arvojournals.org on 08/11/2022

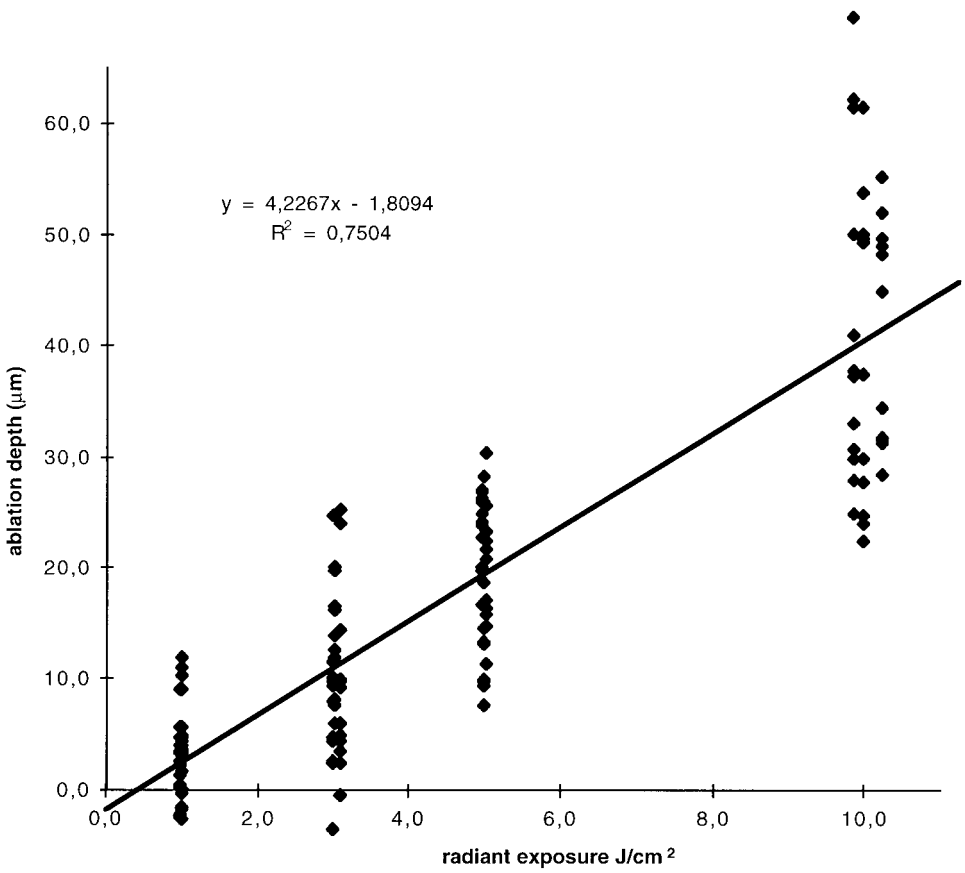

FIGURE 9. Graph depicting the ablation depth for all measured laser spots. The straight line represents the linear regression. $R^2 = 0.7504$.

Agar gel provided some advantages in the processing of retinal tissue where retinal detachment occurred. Besides the fact that it is readily available and inexpensive, agar gel behaves identically to real tissue during routine tissue processing but does not stain with most widely used staining techniques (i.e., hematoxylin and eosin, periodic acid–Schiff, and Masson trichrome). It is therefore possible to process the entire tissue-agar sample in the same way one would process the tissue sample itself.

Light Microscopy and Ablation Depth

In light microscopy sections, multiple artifacts might have been produced during histologic processing, mounting, and staining of the tissue samples. Not only were there differences in thickness of laser-exposed areas but also normal retina displayed great differences in thickness of different layers.

However, the radial fibers of the Mueller cells and the ILM were clearly visible. Thus, miniature changes in the appearance of the ILM could be easily demonstrated. One scale unit of the measuring eyepiece represented a distance of 2.5 μm with the high-power magnification ($\times$40).

Laser ablation of retinal tissue increased with the radiant exposure in a linear fashion. The graphical presentation of our data shows a relatively wide range of tissue ablation for each individual radiant exposure. This could lead to the conclusion of an unprecise ablation of the Er:YAG laser. However, several factors contributed to the wide range of ablation depths.

First, a major impact is related to the distance between the fiber tip and the retina. Although we were able to demonstrate that the variation of the distance could be maintained between 1.0 $\pm$ 0.3 mm, there is still a variation of the radiant exposure of up to $\pm$13%.

Second, miniature vitreous remnants remaining on the retinal surface block infrared wavelengths and reduce the measurable effect on the retina.

An interesting finding that was encountered when histologic sections were studied was that outer photoreceptor segments were distorted and diverted in one direction after irradiation with radiant exposures exceeding 3 J/cm^2. This was commonly observed at the peripheral region of laser-induced areas of retinal ablation. Possible explanations for this phenomenon could be a temperature-induced coagulation or a pressure-induced mechanical distortion of the outer segments. However, a temperature effect seems rather unlikely because photoreceptor outer segments in the center of laser spots do not exhibit such changes. The fact that pressure transients could not be detected within perfluorodecaline does not exclude the possibility of a more static pressure force of rather low amplitude originating from the bubble expansion. Whether this phenomenon is associated with permanent damage of the photoreceptor function is the subject of further in vivo studies.

CONCLUSION

On the basis of our experimental data, precise ablation of epiretinal membranes under perfluorodecaline liquid seems to be possible. The high precision with minimal thermal damage to the adjacent tissue is a result of the strong absorption of 2.94

Downloaded from tvst.arvojournals.org on 08/11/2022

μm radiation in water. By using a perfluorodecaline liquid that exhibits a low absorption of IR-radiation, tissue ablation is possible without creating strong pressure transients, as is the case if ablation is performed in an aqueous environment of the vitreous, saline or blood.

Our findings suggest that a radiant exposure between 1 and 3 J/cm^2 in combination with a pulse duration of 250 μsec and a probe–retinal distance of 1 mm are suitable for precise ablation of retinal tissue.

Acknowledgment

The authors gratefully acknowledge the technical support from Andreas Friedrich.

References

1. Green WR. Chapter 9: Retina. In: Spencer WH, ed. *Ophthalmic Pathology: an atlas and textbook*. 4th ed. Philadelphia: WB Saunders; 1996:773–1331.
2. Weller M, Esser P, Heimann K, Wiedemann P. Die idiopathische proliferative Vitreoretinopathie: Die Aktivierung von Mikrogliazellen als entscheidender Faktor. *Ophthalmologe.* 1992;89:387–390.
3. Kono T, Kohno T, lnomata H. Epiretinal membrane formation: light and electron microscopic study in an experimental rabbit model. *Arch Ophthalmol.* 1995;113:359–363.
4. Heidenkummer HP, Kampik A. Morphologic analysis of epiretinal membranes in surgically treated idiopathic macular foramina: results of light and electron microscopy. *Ophthalmologe.* 1996;99:675–679.
5. Blumenkranz MS, Azen SP, Aaberg T, et al. Relaxing retinotomy with silicone oil or long acting gas in eyes with severe proliferative retinopathy. *Am J Ophthalmol.* 1993;116:557–564.
6. Bovey EH, DeAncos E, Gonvers M. Retinotomies of 180 degrees or more. *Retina.* 1995;15:394–398.
7. Charteris DG. Proliferative vitreoretinopathy: pathobiology, surgical management and adjunctive treatment. *Am J Ophthalmol.* 1995;79:953–960.
8. Kampik A, Kenyon KR, Michels RG, Green WR, de la Cruz ZC. Epiretinal and vitreous membranes: comparative study of 56 cases. *Arch Ophthalmol.* 1981;99:1445–1454.
9. Kono T, Hurukawa H, Higashi M, Akiya S, Kohno T. Experimental studies of retinal glial cell proliferation on retinal surface. *Nippon Ganka Gakkai Zasshi Acta Societatis Ophthalmologicae Japonicae.* 1990;94:333–339.
10. D'Amico DJ, Yarborough J, Theodossiadis PG, Moulton RS. Erbium:YAG laser photothermal retinal ablation in enucleated rabbit eyes. *Am J Ophthalmol.* 1994;117:783–790.
11. D'Amico DJ, Brooks GE, Marcellino GR, et al. Multicenter clinical experience using an erbium:YAG laser for vitreoretinal surgery. *Ophthalmology.* 1996;103:1575–1585.
12. D'Amico DJ, Brazitikos PD, Marcellino GR, Finn SM, Hobart JL. Initial clinical experience with an erbium:YAG laser for vitreoretinal surgery. *Am J Ophthalmol.* 1996;121:414–425.
13. Brazitikos PD, Walsh AW, Bernal MT, D'Amico DJ. Erbium:YAG laser surgery of the vitreous and retina. *Ophthalmology.* 1995;102:278–290.
14. Zweig AD, Meierhofer OM, Müller OM, et al. Lateral thermal damage along pulsed laser incisions. *Lasers Surg Med.* 1990;10:262–274.
15. Bende T, Seiler T, Wollensak J. Photoablation with the ER:YAG laser in ocular tissues. *Fortschritte der Ophthalmologie.* 1991;88:12–16.
16. Zolotarev VM, Mikhailov BA, Alperovich LI, Polov SI. Dispersion and absorption of liquid water in the infrared and radio regions of the spectrum. *Opt Spectrosc.* 1969;27:430–432.
17. Peyman GA, Katoh N. Effects of an erbium:YAG laser on ocular structures. *Int Ophthalmol.* 1987;10:245–253.
18. Margolis TI, Farnath DA, Destro M, Puliafito CA. Erbium-YAG laser surgery on experimental vitreous membranes. *Arch Ophthalmol.* 1989;107:424–428.
19. Tsubota K. Application of erbium:YAG laser in ocular ablation. *Ophthalmologica.* 1990;200:414–425.
20. Frenz M, Pratisto H, Könz F, Jansen ED. Comparison of the effects of absorption coefficient and pulse duration of 2.12 μm and 2.79 μm radiation on laser ablation of tissue. *IEEE J Quantum Electronics.* 1996;32:2025–2036.
21. Frenz M, Pratisto H, Ith M, et al. Transient photoacoustic effects induced in liquids by pulsed erbium laser. *SPIE Proc Laser - Tissue - Interaction.*" 1994;2134:402–412.
22. Jansen ED, Asshauer T, Frenz M, Motamedi M, Delacrétaz G, Welch AJ. Effect of pulse duration on bubble formation and laser-induced pressure waves during holmium laser ablation. *Lasers Surg Med.* 1996;18:278–293.
23. Helfer D. Endoscopic beam delivery system for erbium laser radiation (diploma work thesis). Berne, Switzerland: University of Berne; 1993.
24. Pellin MJ, Williams GA, Young CE. Endoexcimer laser intraocular ablative photodecomposition (letter). *Am J Ophthalmol.* 1985;99:483.
25. Lewis A, Palanker D, Hemo I, Pe' er J, Zauberman H. Microsurgery of the retina with a needle-guided 193-nm excimer laser. *Invest Ophthalmol Vis Sci.* 1992;33:2377–2381.
26. Walch JTJ, Flotte TJ, Deutsch TF. ER:YAG laser ablation of tissue: effects of pulse duration and tissue type on thermal damage. *Lasers Surg Med.* 1989;9:314–326.
27. Frenz M, Pratisto H, Toth C, Jansen ED, Welch AJ, Weber HP. Perfluorocarbon compounds: transmitting liquids for infrared laser-tissue ablation. *SPIE Proc "Laser - Tissue - Interaction VII.* 1996;2681:343–352.
28. Pratisto H, Ith M, Frenz M, Weber HP. Infrared multiwavelength laser system for establishing a surgical delivery path through water. *Appl Phys Lett.* 1995;67:1963–1965.

Downloaded from tvst.arvojournals.org on 08/11/2022